

CHEMICAL PHYSICS

Using *parahydrogen* to hyperpolarize amines, amides, carboxylic acids, alcohols, phosphates, and carbonates

Wissam Iali, Peter J. Rayner, Simon B. Duckett*

Hyperpolarization turns weak nuclear magnetic resonance (NMR) and magnetic resonance imaging (MRI) responses into strong signals, so normally impractical measurements are possible. We use *parahydrogen* to rapidly hyperpolarize appropriate ^1H , ^{13}C , ^{15}N , and ^{31}P responses of analytes (such as NH_3) and important amines (such as phenylethylamine), amides (such as acetamide, urea, and methacrylamide), alcohols spanning methanol through octanol and glucose, the sodium salts of carboxylic acids (such as acetic acid and pyruvic acid), sodium phosphate, disodium adenosine 5'-triphosphate, and sodium hydrogen carbonate. The associated signal gains are used to demonstrate that it is possible to collect informative single-shot NMR spectra of these analytes in seconds at the micromole level in a 9.4-T observation field. To achieve these wide-ranging signal gains, we first use the signal amplification by reversible exchange (SABRE) process to hyperpolarize an amine or ammonia and then use their exchangeable NH protons to relay polarization into the analyte without changing its identity. We found that the ^1H signal gains reach as high as 650-fold per proton, whereas for ^{13}C , the corresponding signal gains achieved in a ^1H - ^{13}C refocused insensitive nuclei enhanced by polarization transfer (INEPT) experiment exceed 570-fold and those in a direct-detected ^{13}C measurement exceed 400-fold. Thirty-one examples are described to demonstrate the applicability of this technique.

INTRODUCTION

Nuclear magnetic resonance (NMR) is one of the most powerful methods for the study of materials, and magnetic resonance imaging (MRI) plays a vital role in clinical diagnosis. However, the low sensitivity of these techniques limits their applicability. The hyperpolarization method dynamic nuclear polarization (DNP) improves the detectability of analytes such as pyruvate to the level that the MRI-based diagnosis of disease is now possible (1). *Parahydrogen* ($p\text{-H}_2$), which is cheap to prepare and exists as a pure nuclear spin state, was shown to enhance the strength of an NMR signal in 1987 (2), although these methods have not yet been used clinically. This may reflect the fact that $p\text{-H}_2$ was originally used to sensitize chemically modified hydrogenation products (3, 4), and only recently has a method been developed where the original identity of the sensitized analyte is retained (5). This approach, signal amplification by reversible exchange (SABRE), harnesses $p\text{-H}_2$ in the form of metal-bound hydride ligands and transfers hyperpolarization into a weakly bound substrate (6–8) via the small J -couplings that connect them (9). Ligand exchange then builds up a pool of hyperpolarized substrate according to Scheme 1A (10). SABRE is successful for analytes with multiple bonds to nitrogen such as nicotinamide (11), isoniazid (12), pyrazole (13), and acetonitrile (14), with ^1H polarizations of 50% (11) and ^{15}N values of 20% (15) being achieved. Furthermore, although it works for other nuclei (11, 16–20), it fails to sensitize many classes of analytes.

Here, we describe a method where $p\text{-H}_2$ hyperpolarizes a range of amines, amides, carboxylic acids, alcohols, phosphates, and carbonates without changing their chemical identity. Our method starts with the hyperpolarization of ammonia (the hyperpolarization transfer agent). Subsequently, polarization is relayed into the specified analyte through proton exchange, as outlined in Scheme 1B. Spontaneous low-field transfer then creates the hyperpolarized analyte, which we detect. We called this approach SABRE-RELAY and predict that, when it is fully optimized, it will have a major impact on NMR and MRI in accordance with the fact that we exemplify it for 31 analytes.

Department of Chemistry, University of York, Heslington, York YO10 5DD, UK.
*Corresponding author. Email: sbd3@york.ac.uk

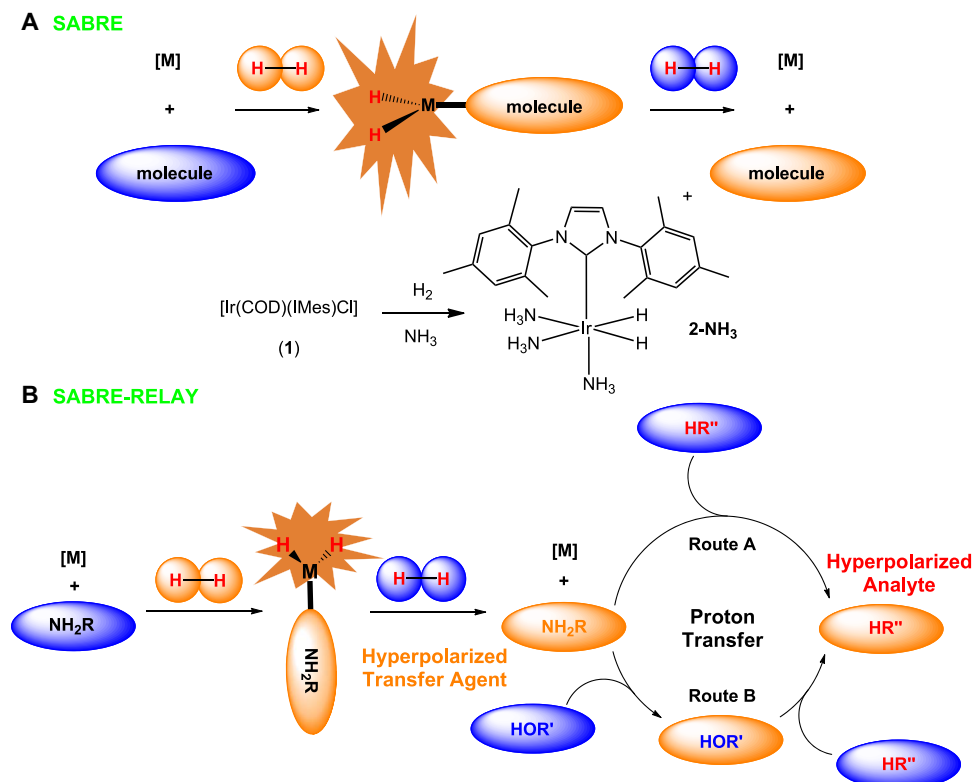
RESULTS

We achieve SABRE-RELAY by reacting ammonia with the most versatile of the current SABRE catalysts, $[\text{IrCl}(\text{COD})(\text{IMes})]$ (21, 22) (1) [where IMes is 1,3-bis(2,4,6-trimethylphenyl)imidazol-2-ylidene and COD is cycloocta-1,5-diene] and H_2 , to form $[\text{Ir}(\text{H})_2(\text{IMes})(\text{NH}_3)_3]\text{Cl}$ (2-NH₃) according to Scheme 1. When this reaction is completed in dichloromethane- d_2 , 2-NH₃ exhibits equatorial and axial NH₃ ligand signals at δ 2.19 and 2.88 in the corresponding ^1H NMR spectrum, alongside a broad NH₃ response at δ 0.47, as detailed in Fig. 1A. When this sample is examined after exposure to a 2-bar pressure of $p\text{-H}_2$ gas at 60 G, the resulting ^1H NMR signal for free NH₃ now shows an ~10-fold signal enhancement per proton, with the bound NH₃ ligand signal at δ 2.19 showing a 3-fold enhanced response. These observations confirm that 2-NH₃ undergoes SABRE to produce hyperpolarized ammonia. When the same process is repeated in methanol- d_4 , 2-NH₃ exhibits a hydride resonance at δ -23.2 that rapidly separates into several components as H-D exchange proceeds to form an array of isotopologues. However, when $p\text{-H}_2$ is used, a hyperpolarized NMR signal is readily seen at δ 5.06 for the exchangeable proton of CD₃OH, which exhibits a 32-fold intensity gain over its thermally equilibrated signal. Therefore, we added a 5% loading of H₂O, relative to iridium, to the CD₂Cl₂ sample and reexamined it. Under these conditions, the free NH₃ signal gain resulting from SABRE proved to increase to 40-fold per proton, whereas the corresponding equatorial ligand signal now showed an 85-fold per proton gain (Fig. 1B). In addition, the free H₂O signal was enhanced by 75-fold per proton, a result that compares well with other solvent signal enhancements (23–25).

Exchange spectroscopy measurements were then used to confirm that free NH₃ and the equatorially bound NH₃ ligand of 2-NH₃ are in chemical exchange, with the observation of further exchange peaks between free NH₃ and H₂O demonstrating the rapid transfer of protons between them. On the basis of this selectivity, we conclude that, when the ammonia is bound, proton exchange between NH₃ and H₂O is suppressed because the nitrogen lone pair is involved in bonding to the metal center. Consequently, it now becomes hyperpolarized by SABRE. Proton exchange proceeds, though, after NH₃ dissociation, and this leads to the observation of hyperpolarization in the chemical exchange-averaged

Copyright © 2018
The Authors, some
rights reserved;
exclusive licensee
American Association
for the Advancement
of Science. No claim to
original U.S. Government
Works. Distributed
under a Creative
Commons Attribution
License 4.0 (CC BY).

Downloaded from <http://advances.sciencemag.org/> on June 23, 2018



Scheme 1. (A) Hyperpolarization via SABRE and (B) hyperpolarization via SABRE-RELAY. SABRE is used to hyperpolarize the transfer agent NH₂R, where R is H or CH₂Ph or CH₂CH₂Ph (etc.), which relays polarization to the analyte (HR'', route A), and R' is amide, carboxyl, phosphate, or alkoxide (etc.). This process involves both proton exchange and spin-spin interactions and may be mediated by an intermediary HOR', where R' is H or suitable scaffold (route B). Center: Reaction scheme shows the formation of SABRE active **2-NH₃**, which leads to NH₃.

response of H₂O (or HOCD₃) according to Scheme 1B. Now, we show how it is possible to harness this proton exchange process to hyperpolarize the NMR signals of a series of added analytes.

First, we consider whether the SABRE hyperpolarization of NH₃ can be relayed into the ¹H and ¹³C responses of a series of alcohols CH₃(CH₂)_nOH (where *n* = 0 to 7). To do this, we prepared a range of dichloromethane-*d*₂ solutions that contained [Ir(H₂)₂(IMes)(NH₃)₃]Cl (**2-NH₃**), NH₃, and 1 μl of each alcohol (typical concentration, 20 mM). After hyperpolarization transfer from *p*-H₂, strong signals resulted in the associated single-scan ¹H NMR spectra, which reached up to 650-fold intensity gains per alcohol CH proton for 1-propanol, averaging at 265 across the series (see the Supplementary Materials). When the same *p*-H₂ transfer process was undertaken and a fully coupled ¹³C NMR measurement was made instead of a ¹H NMR measurement, molecule-diagnostic ¹³C and ¹H-¹³C refocused insensitive nuclei enhanced by polarization transfer (INEPT)-based responses could also be recorded in one scan at 9.4 T for all the alcohols, as illustrated in Fig. 2B for 1-pentanol, with the associated signal gains reaching 570-fold for the C_α signal of 1-hexanol. The SABRE-RELAY effect results in the detection of hyperpolarized NMR signals for all the spin-1/2 nuclei in these molecules. In addition, as with SABRE, the hyperpolarized NMR terms reflect a mixture of longitudinal single-spin and higher-order states, whose relative amplitudes depend on the magnetic field that the sample experiences during the polarization transfer step (16, 26). Furthermore, by reducing the concentrations of these analytes below the concentration of NH₃, it is possible to improve on SABRE-RELAY efficiency. This is beneficial when studying low-concentration analytes because

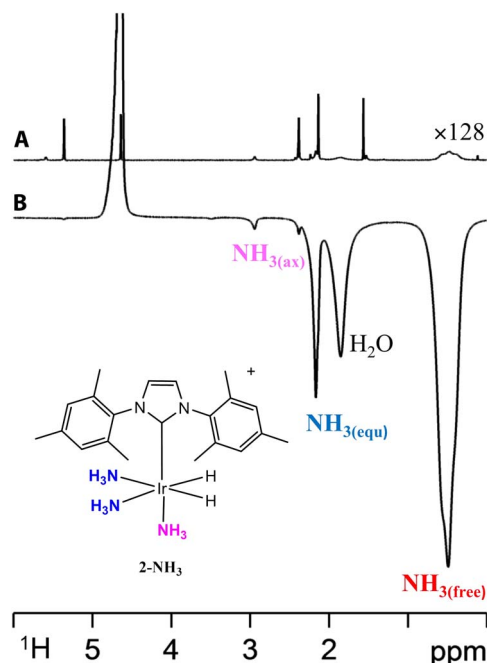


Fig. 1. Hyperpolarization of NH₃ under SABRE. (A) Thermally polarized control ¹H NMR spectrum showing peaks for **2-NH₃**, NH₃, and H₂ at 298 K in dichloromethane-*d*₂, ×128 vertical expansion relative to (B). (B) Corresponding single-scan ¹H NMR spectrum in the presence of *p*-H₂, with the hyperpolarized responses for H₂O, NH₃(free), Ir-NH₃(equatorial), and Ir-NH₃(axial) of **2-NH₃** indicated.

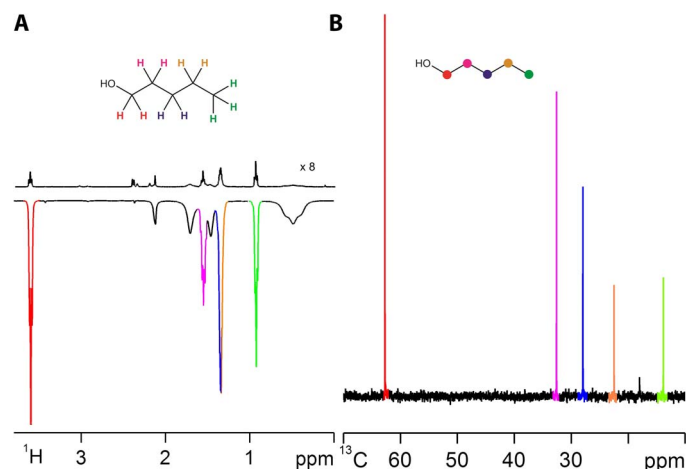


Fig. 2. Single-scan NMR spectra of 15.3 mM pentanol ($\text{CH}_3\text{CH}_2\text{CH}_2\text{CH}_2\text{CH}_2\text{OH}$, color-coded structure shown) in dichloromethane- d_2 solution resulting from the action of NH_3 , 2-NH_3 , and $p\text{-H}_2$. (A) Upper ^1H NMR spectrum in the thermally polarized control, $\times 8$ vertical expansion, relative to lower SABRE-RELAY spectrum. (B) Single-scan SABRE-RELAY ^1H - ^{13}C refocused INEPT NMR spectrum (see fig. S8B for the corresponding thermal control trace).

when propanol was studied, the ^1H NMR signal gains seen for its OH resonance increased by 100% on moving from a 15 to 1.5 mM concentration (fig. S4), whereas its CH resonances showed a ca. 50% improvement in enhancement level; a ^1H - ^{13}C refocused INEPT response was still clearly visible in one scan, where the three signals from the OH end were 639, 538, and 603 times larger, respectively, than those in the corresponding ^{13}C response. This polarization transfer method is also applicable to complex branched alcohols, and when a sample of ^{13}C -labeled glucose was analyzed, a single-scan ^{13}C response could be seen for all the expected α and β form signals, which serves to illustrate the wider significance of this effect (fig. S15E). Furthermore, our studies show that, when SABRE-RELAY is carried out under anhydrous conditions with straight-chain alcohols, superior results are obtained.

Our next goal was to expand on the range of materials that can be sensitized by this method. We started with pyruvic acid but found that its addition to a solution of 2-NH_3 and NH_3 resulted in ammonium salt precipitation, which acted to limit hyperpolarization efficacy. This can be overcome by the addition of a pH modifier such as Cs_2CO_3 , but working with the corresponding sodium salt proved optimal. When ^{13}C -labeled sodium pyruvate, acetate, or propanoic acid samples were studied in the presence of $p\text{-H}_2$, strong ^1H and ^{13}C signals were seen; the ^{13}C signal gain for propionic acid was 109-fold. Furthermore, sodium dihydrogen phosphate, adenosine 5'-triphosphate disodium, and ^{13}C -labeled sodium hydrogen carbonate provided strong ^{31}P and ^{13}C responses (Fig. 3, A and B), whereas the amides acetamide, urea, and methacrylamide showed substantial ^1H , ^{13}C , and ^{15}N signal gains; for urea, a ^{13}C signal gain of 408-fold was observed. These studies could be completed with $\text{NH}_3/\text{H}_2\text{O}$ or $\text{NH}_3/\text{CH}_3\text{OH}$, as detailed in the Supplementary Materials, to promote the necessary proton exchange, and the observations establish that analytes containing the four common functional groups—OH, NH_2CO , POH, and COOH—can be used. In some cases, we see evidence for Schiff-base condensation at long reaction times but could suppress this process by adding water.

To examine the role of the hyperpolarization transfer agent, we replaced NH_3 with benzylamine (BnNH_2) or phenethylamine (PEA).

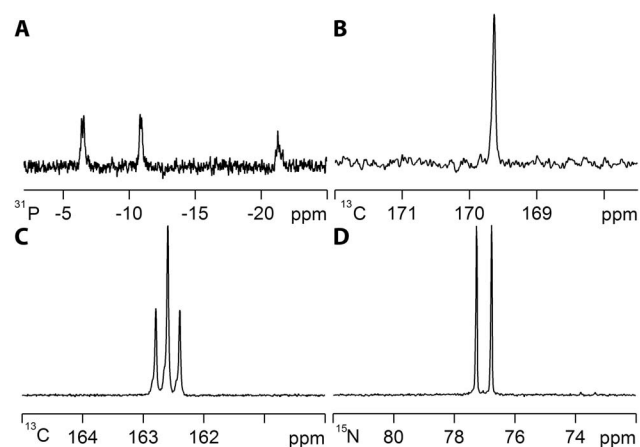


Fig. 3. Single-scan SABRE-RELAY NMR spectra recorded in dichloromethane- d_2 with NH_3 and 2-NH_3 in the presence of $p\text{-H}_2$. (A) Sodium adenosine 5'-triphosphate, ^1H - ^{31}P refocused INEPT spectrum (OH transfer) and (B) sodium ^{13}C -labeled pyruvate, ^{13}C NMR spectrum. Single-scan SABRE-RELAY NMR spectra recorded with PEA and 2-PEA in the presence of $p\text{-H}_2$ for (C) ^{15}N - ^{13}C -labeled urea, ^{13}C NMR spectrum, 25 mM concentration, and (D) ^{15}N - ^{13}C -labeled urea, ^{15}N NMR spectrum, 25 mM concentration. The corresponding thermally polarized spectra are detailed in figs. S29A, S18A, S23A, and S23C and yield no signal.

Both react with **1** and H_2 , forming $[\text{Ir}(\text{H})_2(\text{IMes})(\text{NH}_2\text{Bn})_3]\text{Cl}$ (**2-BnNH₂**) and $[\text{Ir}(\text{H})_2(\text{IMes})(\text{PEA})_3]\text{Cl}$ (**2-PEA**), respectively. For the corresponding **2-BnNH₂** sample, signal gains for free BnNH_2 of 72-fold (NH), 53-fold (CH), and 170-fold (aromatic), respectively, per proton are observed (Fig. 4), and these measurements can be repeated if the same sample is probed with $p\text{-H}_2$ several days after the first observation was made. PEA proved to perform better than BnNH_2 , with the corresponding NH_2 signal gain being 108-fold per proton for a 10-fold loading of **1** with signal gains of 50-fold (NCH_2), 45-fold (CH_2), 92-fold (*ortho*), 50-fold (*meta*), and 20-fold (*para*) resulting for the other groups. These observations show how polarization transfer through the aliphatic carbon chain into the aromatic protons is possible. BnNH_2 and PEA also proved suitable for SABRE-RELAY. In the case of PEA, the efficiency of urea hyperpolarization was found to improve (Fig. 3, C and D) over that achieved with NH_3 , although the measured response of ^{13}C -labeled glucose was found to reduce. Furthermore, replacing BnNH_2 with its *d₇*-form, $\text{C}_6\text{D}_5\text{CD}_2\text{NH}_2$, led to further improvements in observed analyte response level because the initially created SABRE hyperpolarization was now optimally focused into just the NH_2 protons.

Given the wide range of amine $\text{p}K_b$ values (27), it may be possible to remove the need for an auxiliary base when dealing with acidic analytes through a process of amine variation. Therefore, we conclude that studies on the role of the amine will be important for the optimization of SABRE-RELAY and may even allow the introduction of selectivity into the hyperpolarization process. Furthermore, because improvements in analyte detectability with SABRE can be easily achieved by varying the polarization transfer field, reducing relaxation within the analyte, and optimizing the catalyst lifetime while minimizing its relaxivity, we expect the signal gains reported here to be similarly improved upon in the future (5).

DISCUSSION

In summary, we have shown that SABRE-RELAY can be used to hyperpolarize a wide range of biologically relevant materials. In the initial

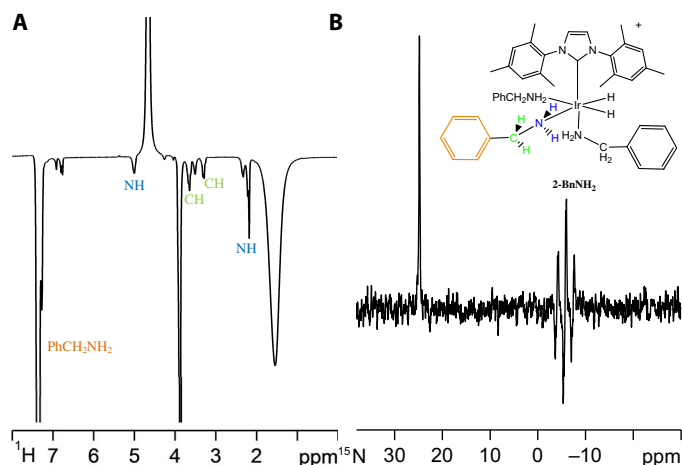


Fig. 4. Hyperpolarization of benzylamine (BnNH₂) under SABRE. (A) ¹H NMR spectrum of hyperpolarized BnNH₂ achieved via **2-BnNH₂** (top right) under SABRE in dichloromethane-*d*₂ solution after transfer at 60 G (see fig. S32A for the corresponding thermally equilibrated NMR spectrum). The enhanced signals are color-coded; NH₂ (blue), CH₂ (light green), and Ph (orange) for the bound equatorial BnNH₂ ligand of **2-BnNH₂**, NH₂ and CH₂ of the free material, and H₂O. (B) Corresponding ¹⁵N NMR spectrum recorded using ¹⁵N-labeled BnNH₂ after transfer in a μ-metal shield showing the free (left) and equatorial ligand (right) responses.

step, SABRE is used to enhance the NH proton response of the selected hyperpolarized transfer agent (the free amine) by between 10- and 120-fold per proton. When this is achieved in the presence of propanol, proton exchange results in its OH signal being amplified by between 250- and 500-fold. The nonequilibrium magnetic state of the OH proton is then successfully relayed into its aliphatic ¹H resonances such that the corresponding signals are amplified by between 650- and 790-fold per proton. We used this ¹H signal gain to record a single-scan ¹H-¹³C refocused INEPT NMR spectrum using just 1×10^{-7} moles of material, although direct transfer to ¹³C means that a weaker fully coupled ¹³C response can also be seen. On the basis of these signal gains, we hope that this route can be developed to allow the phenotyping of urine via lower-field ¹³C detection in the future as an alternative to the current high-field ¹H detection methods (28). However, because exchangeable protons feature heavily in biochemical NMR, we expect harnessing this effect to be of significant interest to biochemists, especially if it is augmented with high-field transfer via the “low-irradiation generation of high tesla-SABRE” approach (29). In addition, because hyperpolarized urea, glucose, and pyruvate reflect successful MRI probes of disease (30, 31), when SABRE-RELAY is coupled with catalyst removal and biocompatibility, we expect this route to become clinically important because it can theoretically deliver a continuously hyperpolarized bolus (32). Moreover, because studies of catalysis with *p*-H₂ have made significant contributions to process optimization (33–37), we expect this approach to provide insight into important reactions such as transfer hydrogenation (38), hydroamination (39), and N₂ fixation in the future (40).

MATERIALS AND METHODS

Experimental design

The measurements undertaken in this work were completed on a 400-MHz Avance III spectrometer and involved ¹H, ¹³C, ¹⁵N, and ³¹P detection, as detailed in the Supplementary Materials. Enhancement values were determined according to the methods defined here,

and sample details allowed the repetition of these measurements, which involved the following procedures.

SABRE-RELAY polarization transfer method with NH₃

The polarization transfer experiments that were reported in this study were conducted in 5-mm NMR tubes that were equipped with a J. Young’s tap. Samples for these polarization transfer experiments were based on a 5 mM solution of [IrCl(COD)(IMes)] and the indicated substrate and NH₃ loadings in methanol-*d*₄ or dichloromethane-*d*₂ (0.6 ml). The samples were degassed before the introduction of NH₃. Subsequently, *p*-H₂ at a pressure of ca. 3 bar was added. Then, samples were shaken for 10 s in the specified fringe field of an NMR spectrometer before they were rapidly transported into the magnet for subsequent interrogation by NMR spectroscopy. This whole process takes ca. 15 s to achieve.

SABRE-RELAY polarization transfer method with BnNH₂ or PEA

The polarization transfer experiments that were reported were conducted in 5-mm NMR tubes that were equipped with a J. Young’s tap. Samples for these polarization transfer experiments were based on a 5 mM solution of [IrCl(COD)(IMes)], the indicated BnNH₂ or PEA loading, and the indicated additional substrate at the specified loading in dichloromethane-*d*₂ (0.6 ml). The samples were degassed before the introduction of *p*-H₂ at a pressure of ca. 3 bar. Samples were then shaken for 10 s in the specified fringe field of an NMR spectrometer before they were rapidly transported into the magnet for subsequent interrogation by NMR spectroscopy.

SUPPLEMENTARY MATERIALS

Supplementary material for this article is available at <http://advances.sciencemag.org/cgi/content/full/4/1/eaao6250/DC1>

- section S1. SABRE-RELAY polarization transfer method with NH₃
- section S2. SABRE-RELAY polarization transfer method with BnNH₂ or PEA
- section S3. Polarization enhancement quantification procedures
- section S4. NMR spectrometer details
- section S5. Pulse sequence details
- section S6. SABRE-RELAY spectra
- fig. S1. INEPT pulse sequence.
- fig. S2. DEPT pulse sequence.
- fig. S3. SABRE-RELAY NMR spectra methanol.
- fig. S4. SABRE-RELAY NMR spectra ethanol.
- fig. S5. SABRE-RELAY NMR spectra propanol.
- fig. S6. SABRE-RELAY NMR spectra propanol, low concentration.
- fig. S7. SABRE-RELAY NMR spectra butanol.
- fig. S8. SABRE-RELAY NMR spectra pentanol.
- fig. S9. SABRE-RELAY NMR spectra hexanol.
- fig. S10. SABRE-RELAY NMR spectra heptanol.
- fig. S11. SABRE-RELAY NMR spectra octanol.
- fig. S12. SABRE-RELAY NMR spectra isopropanol.
- fig. S13. SABRE-RELAY NMR spectra *tert*-butanol.
- fig. S14. SABRE-RELAY NMR spectra *D*-glucose.
- fig. S15. SABRE-RELAY NMR spectra *D*-glucose-¹³C.
- fig. S16. SABRE-RELAY NMR spectra glycerol.
- fig. S17. SABRE-RELAY NMR spectra sodium acetate-¹³C.
- fig. S18. SABRE-RELAY NMR spectra sodium pyruvate-¹³C.
- fig. S19. SABRE-RELAY NMR spectra sodium acetate-1,2-¹³C₂.
- fig. S20. SABRE-RELAY NMR spectra propionic acid-¹³C.
- fig. S21. SABRE-RELAY NMR spectra sodium hydrogen carbonate-¹³C.
- fig. S22. SABRE-RELAY NMR spectra urea-¹³C.
- fig. S23. SABRE-RELAY NMR spectra urea-¹³C-¹⁵N₂.
- fig. S24. SABRE-RELAY NMR spectra urea-¹³C-¹⁵N₂.
- fig. S25. SABRE-RELAY NMR spectra acetamide.
- fig. S26. SABRE-RELAY NMR spectra methacrylamide.
- fig. S27. SABRE-RELAY NMR spectra cyclohexyl methacrylamide.
- fig. S28. SABRE-RELAY NMR spectra mono sodium dihydrogen orthophosphate.

fig. S29. SABRE-RELAY NMR spectra adenosine 5'-triphosphate disodium salt.
 fig. S30. SABRE-RELAY NMR spectra ammonia in methanol.
 fig. S31. SABRE-RELAY NMR spectra ammonia in dichloromethane.
 fig. S32. SABRE-RELAY NMR spectra benzylamine.
 fig. S33. SABRE-RELAY NMR spectra benzylamine-¹⁵N.
 fig. S34. SABRE-RELAY NMR spectra, mixture of urea, propanol, and PEA.
 table S1. Alcohol ¹H SABRE-RELAY signal enhancement values.
 table S2. Alcohol ¹³C SABRE-RELAY signal enhancement values.
 table S3. NMR data for **2-NH₃**.
 table S4. NMR data for **2-BnNH₂**.

REFERENCES AND NOTES

- J. H. Ardenkjaer-Larsen, On the present and future of dissolution-DNP. *J. Magn. Reson.* **264**, 3–12 (2016).
- C. R. Bowers, D. P. Weitekamp, Parahydrogen and synthesis allow dramatically enhanced nuclear alignment. *J. Am. Chem. Soc.* **109**, 5541–5542 (1987).
- J. Natterer, J. Bargon, Parahydrogen induced polarization. *Prog. Nucl. Magn. Reson. Spectrosc.* **31**, 293–315 (1997).
- R. A. Green, R. W. Adams, S. B. Duckett, R. E. Mewis, D. C. Williamson, G. G. R. Green, The theory and practice of hyperpolarization in magnetic resonance using parahydrogen. *Prog. Nucl. Magn. Reson. Spectrosc.* **67**, 1–48 (2012).
- R. W. Adams, J. A. Aguilar, K. D. Atkinson, M. J. Cowley, P. I. P. Elliott, S. B. Duckett, G. G. R. Green, I. G. Khazal, J. López-Serrano, D. C. Williamson, Reversible interactions with para-hydrogen enhance NMR sensitivity by polarization transfer. *Science* **323**, 1708–1711 (2009).
- R. W. Adams, S. B. Duckett, R. A. Green, D. C. Williamson, G. G. R. Green, A theoretical basis for spontaneous polarization transfer in non-hydrogenative parahydrogen-induced polarization. *J. Chem. Phys.* **131**, 194505 (2009).
- A. N. Pravdivtsev, A. V. Yurkovskaya, H. M. Vieth, K. L. Ivanov, R. Kaptein, Level anti-crossings are a key factor for understanding para-hydrogen-induced hyperpolarization in SABRE experiments. *ChemPhysChem* **14**, 3327–3331 (2013).
- A. N. Pravdivtsev, A. V. Yurkovskaya, K. L. Ivanov, H.-M. Vieth, Importance of polarization transfer in reaction products for interpreting and analyzing CIDNP at low magnetic fields. *J. Magn. Reson.* **254**, 35–47 (2015).
- N. Eshuis, R. L. E. G. Aspers, B. J. A. van Weerdenburg, M. C. Feiters, F. P. J. T. Rutjes, S. S. Wijmenga, M. Tessari, Determination of long-range scalar ¹H–¹H coupling constants responsible for polarization transfer in SABRE. *J. Magn. Reson.* **265**, 59–66 (2016).
- K. D. Atkinson, M. J. Cowley, P. I. P. Elliott, S. B. Duckett, G. G. R. Green, J. López-Serrano, A. C. Whitwood, Spontaneous transfer of parahydrogen derived spin order to pyridine at low magnetic field. *J. Am. Chem. Soc.* **131**, 13362–13368 (2009).
- P. J. Rayner, M. J. Burns, A. M. Olaru, P. Norcott, M. Fekete, G. G. R. Green, L. A. R. Highton, R. E. Mewis, S. B. Duckett, Delivering strong ¹H nuclear hyperpolarization levels and long magnetic lifetimes through signal amplification by reversible exchange. *Proc. Natl. Acad. Sci. U.S.A.* **114**, E3188–E3194 (2017).
- H. Zeng, J. Xu, J. Gillen, M. T. McMahon, D. Artemov, J.-M. Tyburn, J. A. B. Lohman, R. E. Mewis, K. D. Atkinson, G. G. R. Green, S. B. Duckett, P. C. M. van Zijl, Optimization of SABRE for polarization of the tuberculosis drugs pyrazinamide and isoniazid. *J. Magn. Reson.* **237**, 73–78 (2013).
- E. B. Ducker, L. T. Kuhn, K. Münnemann, C. Griesinger, Similarity of SABRE field dependence in chemically different substrates. *J. Magn. Reson.* **214**, 159–165 (2012).
- R. E. Mewis, R. A. Green, M. C. R. Cockett, M. J. Cowley, S. B. Duckett, G. G. R. Green, R. O. John, P. J. Rayner, D. C. Williamson, Strategies for the hyperpolarization of acetonitrile and related ligands by SABRE. *J. Phys. Chem. B* **119**, 1416–1424 (2015).
- D. A. Barskiy, R. V. Shchepin, A. M. Coffey, T. Theis, W. S. Warren, B. M. Goodson, E. Y. Chekmenev, Over 20% ¹⁵N hyperpolarization in under one minute for metronidazole, an antibiotic and hypoxia probe. *J. Am. Chem. Soc.* **138**, 8080–8083 (2016).
- R. E. Mewis, K. D. Atkinson, M. J. Cowley, S. B. Duckett, G. G. R. Green, R. A. Green, L. A. R. Highton, D. Kilgour, L. S. Lloyd, J. A. B. Lohman, D. C. Williamson, Probing signal amplification by reversible exchange using an NMR flow system. *Magn. Reson. Chem.* **52**, 358–369 (2014).
- J. F. P. Colell, A. W. J. Logan, Z. Zhou, R. V. Shchepin, D. A. Barskiy, G. X. Ortiz Jr., Q. Wang, S. J. Malcolmson, E. Y. Chekmenev, W. S. Warren, T. Theis, Generalizing, extending, and maximizing nitrogen-15 hyperpolarization induced by parahydrogen in reversible exchange. *J. Phys. Chem. C* **121**, 6626–6634 (2017).
- D. A. Barskiy, R. V. Shchepin, C. P. N. Tanner, J. F. P. Colell, B. M. Goodson, T. Theis, W. S. Warren, E. Y. Chekmenev, The absence of quadrupolar nuclei facilitates efficient ¹³C hyperpolarization via reversible exchange with parahydrogen. *ChemPhysChem* **18**, 1493–1498 (2017).
- V. V. Zhivonitko, I. V. Skovpin, I. V. Koptuyug, Strong ³¹P nuclear spin hyperpolarization produced via reversible chemical interaction with parahydrogen. *Chem. Commun.* **51**, 2506–2509 (2015).
- M. J. Burns, P. J. Rayner, G. G. R. Green, L. A. R. Highton, R. E. Mewis, S. B. Duckett, Improving the hyperpolarization of ³¹P nuclei by synthetic design. *J. Phys. Chem. B* **119**, 5020–5027 (2015).
- B. J. A. van Weerdenburg, S. Glöggler, N. Eshuis, A. H. J. T. Engwerda, J. M. M. Smits, R. de Gelder, S. Appelt, S. S. Wijmenga, M. Tessari, M. C. Feiters, B. Blümich, F. P. J. T. Rutjes, Ligand effects of NHC–iridium catalysts for signal amplification by reversible exchange (SABRE). *Chem. Commun.* **49**, 7388–7390 (2013).
- L. S. Lloyd, A. Asghar, M. J. Burns, A. Charlton, S. Coombes, M. J. Cowley, G. J. Dear, S. B. Duckett, G. R. Genov, G. G. R. Green, L. A. R. Highton, A. J. J. Hooper, M. Khan, I. G. Khazal, R. J. Lewis, R. E. Mewis, A. D. Roberts, A. J. Ruddlesden, Hyperpolarisation through reversible interactions with parahydrogen. *Cat. Sci. Technol.* **4**, 3544–3554 (2014).
- S. Lehmkuhl, M. Emondts, L. Schubert, P. Spanning, J. Klankermayer, B. Blümich, P. P. M. Schleker, Hyperpolarizing water with parahydrogen. *ChemPhysChem* **18**, 2426–2429 (2017).
- K. X. Moreno, K. Nasr, M. Milne, A. D. Sherry, W. J. Goux, Nuclear spin hyperpolarization of the solvent using signal amplification by reversible exchange (SABRE). *J. Magn. Reson.* **257**, 15–23 (2015).
- M. Fekete, P. J. Rayner, G. G. R. Green, S. B. Duckett, Harnessing polarisation transfer to indazole and imidazole through signal amplification by reversible exchange to improve their NMR detectability. *Magn. Reson. Chem.* **55**, 944–957 (2017).
- M. L. Truong, T. Theis, A. M. Coffey, R. V. Shchepin, K. W. Waddell, F. Shi, B. M. Goodson, W. S. Warren, E. Y. Chekmenev, ¹⁵N hyperpolarization by reversible exchange using SABRE-SHEATH. *J. Phys. Chem. C* **119**, 8786–8797 (2015).
- H. K. Hall Jr., Correlation of the base strengths of amines¹. *J. Am. Chem. Soc.* **79**, 5441–5444 (1957).
- O. Beckonert, H. C. Keun, T. M. D. Ebbels, J. G. Bundy, E. Holmes, J. C. Lindon, J. K. Nicholson, Metabolic profiling, metabolomic and metabonomic procedures for NMR spectroscopy of urine, plasma, serum and tissue extracts. *Nat. Protoc.* **2**, 2692–2703 (2007).
- T. Theis, M. Truong, A. M. Coffey, E. Y. Chekmenev, W. S. Warren, LIGHT-SABRE enables efficient in-magnet catalytic hyperpolarization. *J. Magn. Reson.* **248**, 23–26 (2014).
- S. Månsson, E. Johansson, P. Magnusson, C.-M. Chai, G. Hansson, J. S. Petersson, F. Ståhlberg, K. Golman, ¹³C imaging—A new diagnostic platform. *Eur. Radiol.* **16**, 57–67 (2006).
- J. Kurhanewicz, D. B. Vigneron, K. Brindle, E. Y. Chekmenev, A. Comment, C. H. Cunningham, R. J. DeBerardinis, G. G. Green, M. O. Leach, S. S. Rajan, R. R. Rizi, B. D. Ross, W. S. Warren, C. R. Malloy, Analysis of cancer metabolism by imaging hyperpolarized nuclei: Prospects for translation to clinical research. *Neoplasia* **13**, 81–97 (2011).
- J.-B. Hövener, N. Schwaderlapp, T. Lickert, S. B. Duckett, R. E. Mewis, L. A. R. Highton, S. M. Kenny, G. G. R. Green, D. Leibfritz, J. G. Korvink, J. Hennig, D. von Elverfeldt, A hyperpolarized equilibrium for magnetic resonance. *Nat. Commun.* **4**, 2946 (2013).
- O. G. Salnikov, K. V. Kovtunov, D. A. Barskiy, A. K. Khudorozhkov, E. A. Inozemtseva, I. P. Prosvirin, V. I. Bukhtiyarov, I. V. Koptuyug, Evaluation of the mechanism of heterogeneous hydrogenation of α,β -unsaturated carbonyl compounds via pairwise hydrogen addition. *ACS Catal.* **4**, 2022–2028 (2014).
- C. Godard, S. B. Duckett, S. Polas, R. Tooze, A. C. Whitwood, An NMR study of cobalt-catalyzed hydroformylation using para-hydrogen induced polarisation. *Dalton Trans.* 2496–2509 (2009).
- D. J. Fox, S. B. Duckett, C. Flaschenriem, W. W. Brennessel, J. Schneider, A. Gunay, R. Eisenberg, A model iridium hydroformylation system with the large bite angle ligand xantphos: Reactivity with parahydrogen and implications for hydroformylation catalysis. *Inorg. Chem.* **45**, 7197–7209 (2006).
- D. Blazina, S. B. Duckett, P. J. Dyson, J. A. B. Lohman, Direct comparison of hydrogenation catalysis by intact versus fragmented triruthenium clusters. *Angew. Chem. Int. Ed.* **40**, 3874–3877 (2001).
- S. A. Colebrooke, S. B. Duckett, J. A. B. Lohman, R. Eisenberg, Hydrogenation studies involving halobis(phosphine)-ruthenium(I) dimers: Use of parahydrogen induced polarisation to detect species present at low concentration. *Chemistry* **10**, 2459–2474 (2004).
- J. S. M. Samec, J.-E. Bäckvall, P. G. Andersson, P. Brandt, Mechanistic aspects of transition metal-catalyzed hydrogen transfer reactions. *Chem. Soc. Rev.* **35**, 237–248 (2006).
- M. Patel, R. K. Saunthwal, A. K. Verma, Base-mediated hydroamination of alkynes. *Acc. Chem. Res.* **50**, 240–254 (2017).
- J. S. Anderson, J. Rittle, J. C. Peters, Catalytic conversion of nitrogen to ammonia by an iron model complex. *Nature* **501**, 84–87 (2013).

Acknowledgments: We thank A. J. Holmes, M. Fekete, and A. Ruddlesden for their help. **Funding:** We thank the Wellcome Trust (092506 and 098335), the Engineering and Physical Sciences Research Council (EP/R51181X/1), and the University of York for supporting this work. **Author contributions:** W.I., P.J.R., and S.B.D. all contributed equally to the preparation of this manuscript. W.I. and P.J.R. collected the raw data, and all authors were involved in the interpretation of results

and design of experiments. **Competing interests:** W.I., P.J.R., and S.B.D. are inventors on a patent application filed by the University of York based on this work (patent no. GB 1711967.8, filed 25 July 2017). The authors declare that they have no other competing interests. **Data and materials availability:** All data needed to evaluate the conclusions in the paper are present in the paper and/or the Supplementary Materials. All relevant plasmids and experimental data may be requested from the authors. Raw data can be found via DOI: 10.15124/d93f83bf-9fc7-4cf8-8267-504a0304a516.

Submitted 9 August 2017
Accepted 29 November 2017
Published 5 January 2018
10.1126/sciadv.aao6250

Citation: W. Iali, P. J. Rayner, S. B. Duckett, Using *parahydrogen* to hyperpolarize amines, amides, carboxylic acids, alcohols, phosphates, and carbonates. *Sci. Adv.* **4**, eaao6250 (2018).

Using *parahydrogen* to hyperpolarize amines, amides, carboxylic acids, alcohols, phosphates, and carbonates

Wissam Iali, Peter J. Rayner and Simon B. Duckett

Sci Adv 4 (1), eaao6250.
DOI: 10.1126/sciadv.aao6250

ARTICLE TOOLS	http://advances.sciencemag.org/content/4/1/eaao6250
SUPPLEMENTARY MATERIALS	http://advances.sciencemag.org/content/suppl/2017/12/22/4.1.eaao6250.DC1
REFERENCES	This article cites 39 articles, 2 of which you can access for free http://advances.sciencemag.org/content/4/1/eaao6250#BIBL
PERMISSIONS	http://www.sciencemag.org/help/reprints-and-permissions

Use of this article is subject to the [Terms of Service](#)

Science Advances (ISSN 2375-2548) is published by the American Association for the Advancement of Science, 1200 New York Avenue NW, Washington, DC 20005. 2017 © The Authors, some rights reserved; exclusive licensee American Association for the Advancement of Science. No claim to original U.S. Government Works. The title *Science Advances* is a registered trademark of AAAS.